JOURNAL OF GEOPHYSICAL RESEARCH, VOL. 111, D24109, doi:10.1029/2005JD006987, 2006

Terrestrial gamma ray flashes observed aboard the Compton Gamma Ray Observatory/Burst and Transient Source Experiment and ELF/VLF radio atmospherics

M. B. Cohen,[1] U. S. Inan,[1] and G. Fishman[2]

Received 13 December 2005; revised 9 August 2006; accepted 22 August 2006; published 21 December 2006.

[1] During its 9-year lifetime in orbit, the Burst and Transient Source Experiment (BATSE) detector, aboard the Compton Gamma Ray Observatory (CGRO) spacecraft, observed a total of 76 terrestrial gamma ray flashes (TGFs). Of these, simultaneous broadband ELF/VLF data from Palmer Station, Antarctica, were found to be available for six new TGF cases in addition to two previously reported cases (Inan et al., 1996). Analysis of temporal and directional association between radio atmospherics and TGFs reveals solid evidence of an associated radio atmospheric in three of the six events. In one of the three cases with associated radio atmospherics, three consecutive TGFs are apparently linked to three consecutive radio atmospherics. A fourth case exhibits possible evidence of geomagnetically conjugate source lightning. Statistical analyses indicate that when TGFs occur in association with a lightning discharge, they occur ~1–3 ms after the causative lightning event.

Citation: Cohen, M. B., U. S. Inan, and G. Fishman (2006), Terrestrial gamma ray flashes observed aboard the Compton Gamma Ray Observatory/Burst and Transient Source Experiment and ELF/VLF radio atmospherics, *J. Geophys. Res.*, *111*, D24109, doi:10.1029/2005JD006987.

1. Introduction

[2] Although the possibility of gamma emissions at high altitudes above thunderstorms were first suggested as early as 1925 [*Wilson*, 1925], terrestrial gamma ray flashes were first observed in the early 1990s with the Burst and Transient Source Experiment (BATSE) detector, on board the Compton Gamma Ray Observatory (CGRO) [*Fishman et al.*, 1994]. During the 9-year lifetime of the CGRO only 76 TGFs were recorded (~1 per month). The BATSE detector remained the only definitive source of these events until the recent observations of TGFs on the RHESSI spacecraft [*Smith et al.*, 2005].

[3] Nominal results from the RHESSI spacecraft have recently raised the question of the relative timing of the TGF occurrence in comparison to the lightning stroke, indicating that the TGF leads the lightning stroke by 2–5 ms [*Cummer et al.*, 2005; *Stanley et al.*, 2006]. However, the absolute timing of the RHESSI clock is currently in question, and is believed to be known only with 3 ms accuracy. In fact, comparisons with another spacecraft suggest a 3 ms offset (D. M. Smith, private communication, 2005). The independent data set from the BATSE instrument as discussed here may thus prove valuable in assessing this possibility.

[4] Cloud-to-ground lightning discharges radiate a significant fraction of their electromagnetic energy in the ELF/VLF range, from 30 Hz to 30 kHz [*Uman*, 1987, p. 119]. The radiated electromagnetic energy propagates outward from the source, is efficiently guided by the Earth-ionosphere waveguide, and propagates at a velocity close to the speed of light, with typical loss rates of only a few dB per Megameter [*Davies*, 1990, p. 389]. Because of the low attenuation, these so-called radio atmospherics (or sferics for short) emitted by lightning discharges can be detected remotely at global distances (thousands of km) from the source.

[5] Though typical VLF receivers can pick up dozens of sferics every second, here we want to study the specific ones that are associated with TGFs. In this paper, we examine broadband ELF/VLF recordings made at Palmer Station, Antarctica, during the times at which TGFs have been observed on BATSE/CGRO.

2. Description of Data

[6] Continuous, broadband ELF/VLF recordings are made at Palmer Station, Antarctica, for nine hours per day on most days. These high-sensitivity recordings consist of the wideband (100 Hz to 16 kHz) waveforms of electromagnetic fields measured with two orthogonal wire-loop air-core antennas, oriented (prior to 2001) in the geomagnetic north-south (N/S) and east-west (E/W) directions, respectively. Using well established methods of direction

[1]Space, Telecommunications, and Radioscience Laboratory, Stanford University, Stanford, California, USA.
[2]NASA Marshall Space Flight Center, Huntsville, Alabama, USA.

0148-0227/06/2005JD006987$09.00

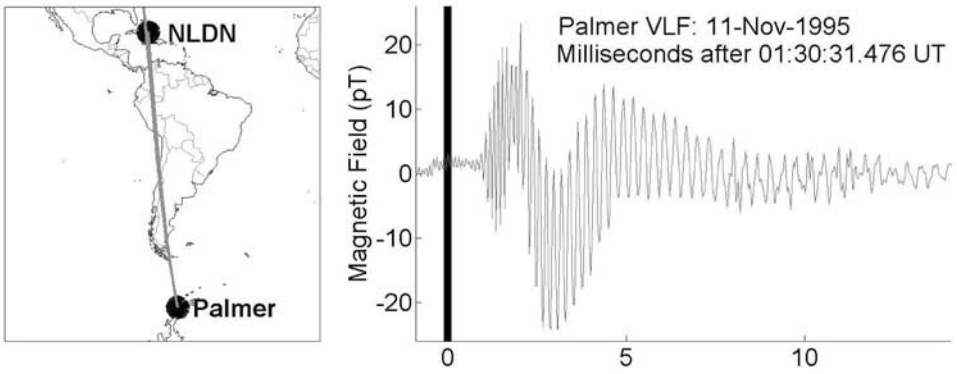

Figure 1. An NLDN recorded lightning stroke, with corresponding sferic arrival at Palmer Station. The vertical line in the VLF data indicates the calculated speed-of-light arrival time, which is less than the 1 ms error of IRIG-B based timing. Direction finding analysis on the sferic places it within 1° of the azimuth corresponding to the NLDN location.

finding [*Wood and Inan*, 2002], and for sferics arriving over global distances of up to 10 Mm, the arrival azimuth can be determined, with accuracy of ~1–2° [*Wood and Inan*, 2004]. In general, 180° ambiguity exists because of the fact that a sferic arriving from the north would be indistinguishable from one arriving from the south. However, the location of Palmer, at the tip of the Antarctic peninsula (64°46′S, 64°03′W), is such that sferics arriving from the south would have to have originated in the continental areas in the Eastern Hemisphere (Australia, Pacific rim and Africa) and would have to propagate over the Antarctic ice cap, and would thus be rapidly attenuated. In this connection, it is important to note that the air over the Antarctic continent itself is extremely dry, so that no lightning occurs in this region. Accordingly, the correct arrival direction can usually be determined in spite of the inherent 180° ambiguity, and observations at Palmer Station thus allow unambiguous detection of sferics over most of the Western Hemisphere.

[7] The timing standard used for the Palmer ELF/VLF recordings during the period of time we reference is a GPS derived IRIG-B timestamp, which provides inherent timing accuracy of ~1 ms. (At the present time Palmer recordings are made with 100 kHz GPS timing, having an inherent accuracy of ~200 ns.) The precise timing of Palmer Station ELF/VLF data can also be confirmed by comparison with the National Lightning Detection Network (NLDN) [*Cummins et al.*, 1998]. Figure 1 shows the correspondence between an NLDN-recorded flash and a radio atmospheric detected at Palmer Station, with a high degree of accuracy (~1–2° azimuth, and <1 ms in time).

[8] It is often useful to separately determine the intensity of sferics, in the ELF and VLF frequency ranges, in order to bring out the particular aspects of lightning flashes that lead to the production of high-altitude effects. The VLF intensity was in past work measured by taking the peak magnetic field in the range 7.5–10 kHz [*Reising et al.*, 1996], but here that frequency range is changed to 5.5–9.5 kHz because of Palmer Station's proximity to the US Navy's Omega navigation beacon in Golfo Nuevo, Argentina, in the 10–14 kHz range (which no longer operates). The VLF frequencies of the sferics are dominated by low-order qTE and qTM waveguide modes, traveling approximately at the speed of light. The peak VLF intensity is known to be closely related to the peak current of the lightning discharge [*Reising et al.*, 1996], as recorded (for example) by NLDN. The ELF energy content of a radio atmospheric has been previously defined as the average magnetic field intensity at frequencies below 1.0 kHz for 10 ms following the sferic [*Reising et al.*, 1996]. In our analyses, because of the fact that the Palmer data was recorded after some high-pass filtering, we use the frequency range 150 Hz to 1.5 kHz, and take the average over 8 ms. The upper cutoff of 1.5 kHz is chosen to be below the lowest waveguide cutoff frequencies for the qTE or qTE modes, so that only the wave energy propagating in the qTEM mode of the Earth-ionosphere waveguide is represented. The ELF energy, thus measured, is closely linked to the total charge moment [*Cummer and Inan*, 1997]. ELF content radiated in qTEM modes attenuates more rapidly with distance than wave energy in the VLF range, and propagates with a group velocity of ~0.9c, creating a sferic characteristic known as a "slow tail" [*Reising et al.*, 1996].

[9] The BATSE instrument consists of eight independent detectors that are sensitive to gamma rays with >~25 keV energy. The BATSE instrument was one of four instruments on the Compton Gamma Ray Observatory that, from April 1991 until June 2000, was in orbital altitude between 350 km and 450 km [*Fishman et al.*, 1994]. The BATSE detectors were designed with substantial down time (~90 minutes) after every trigger, and the thresholds were set for events large enough over an observing period of 32 or 64 ms (appropriate for typical durations of gamma ray bursts of extraterrestrial origin). Hence BATSE is believed to have missed many more TGFs (with much shorter typical durations of ~1 ms) than it recorded, a fact that has now been confirmed by the much larger number of events observed on RHESSI [*Smith et al.*, 2005].

[10] Of the 76 TGF events documented by CGRO, Palmer Station data was serendipitously available for 16 cases. No dedicated recordings were made for the purpose of this collaboration, since the information from the BATSE/CGRO on the detection TGFs was not available in real time. Eight of the 16 cases occurred when BATSE/

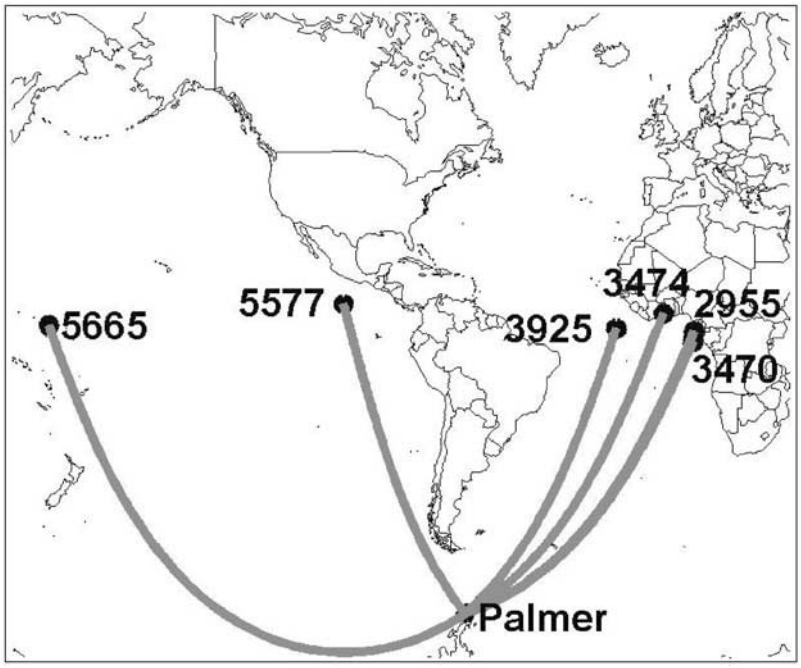

Figure 2. A map showing the locations of the six BATSE TGF cases analyzed here, with great circle paths to Palmer Station.

CGRO was in locations such that the sferic propagation path to Palmer Station crossed the Antarctic ice cap. Sferics propagating over the polar ice cap regions are attenuated much more rapidly. No evidence of a causative sferic could be found, though this result is likely due to the large propagation losses. The eight BATSE trigger numbers for these TGFs are 2370, 2457, 2465, 2808, 3478, 7844, 8083, and 8108.

[11] Two of the remaining eight cases (events 2348 and 3274) were analyzed in an earlier paper [*Inan et al.*, 1996]. Event 2348 was found to be associated with a particularly intense causative lightning discharge arriving from the direction of the CGRO, showing a ''slow tail'' property similar to those associated with sprites. The case of 3274 was found to be inconclusive with regards to lightning association. The remaining six examples for which Palmer ELF/VLF data is available are analyzed in the present paper. Three of the six cases presented here are found to be accompanied with associated radio atmospherics apparently originating from the area of CGRO (3470, 3474, 3925). A fourth case shows some evidence of radio atmospherics originating from the geomagnetically conjugate location to CGRO (5577). For the remaining two TGFs (2955 and 5665) we do find evidence of thunderstorm activity in the region underneath CGRO, there is no evidence of an individual radio atmospheric associated with the TGF observed at Palmer Station. Figure 2 shows the six relevant locations of CGRO at the times it recorded the BATSE TGFs discussed herein, as well as the great circle propagation paths from these locations to Palmer.

3. Geometry of TGFs and Sferics

[12] High-resolution broadband ELF/VLF data for the period of the CGRO/BATSE observations was available from only one location, Palmer Station, thus allowing the determination of only a single arrival azimuth, i.e., direction along a great circle line from which the source lightning discharge is located. It is thus not possible here to determine the geolocation of the source lightning discharges via triangulation based on ELF/VLF measurements at multiple sites [*Wood and Inan*, 2004].

[13] Figure 3 shows the geometry of TGF and sferic detection, including the detection footprint of CGRO. For each TGF case, the source is first assumed to be located immediately below BATSE (i.e., at the radial footprint of the spacecraft), and the expected arrival time to Palmer Station is calculated on the basis of this assumption. Both the propagation time of sferic to Palmer station, and gamma rays to CGRO, are accounted for. The reference time so calculated is referred to here as ''time-zero.'' If our starting assumption is correct, and the TGF occurred simultaneous with the sferic, we expect the onset of the sferic to be at time-zero, arriving from azimuth-zero.

[14] Ostensibly, however, we recognize that the TGF emission could actually have originated from anywhere within the 2700 km (diameter) line-of-sight footprint, though this represents a worst case. The effective detection circle is likely smaller, described by a probability distribution exhibiting a maximum at the nadir point. For an assumed detection radius and shape, it is possible to determine the expected variance in arrival times and directions by integrating the occurrence probability over the region. (Conversely, for a large number of events, it may be possible to invert the arrival distributions to determine the detection footprint of the spacecraft, but this cannot be done here.) Assuming Gaussian detection circles of radius between 100 km and 1000 km (defining the radius as 2σ) yields arrival time distribution means of -0.01 ms and -0.75 ms, and with standard deviations of 0.1 ms and 1.3 ms, respectively.

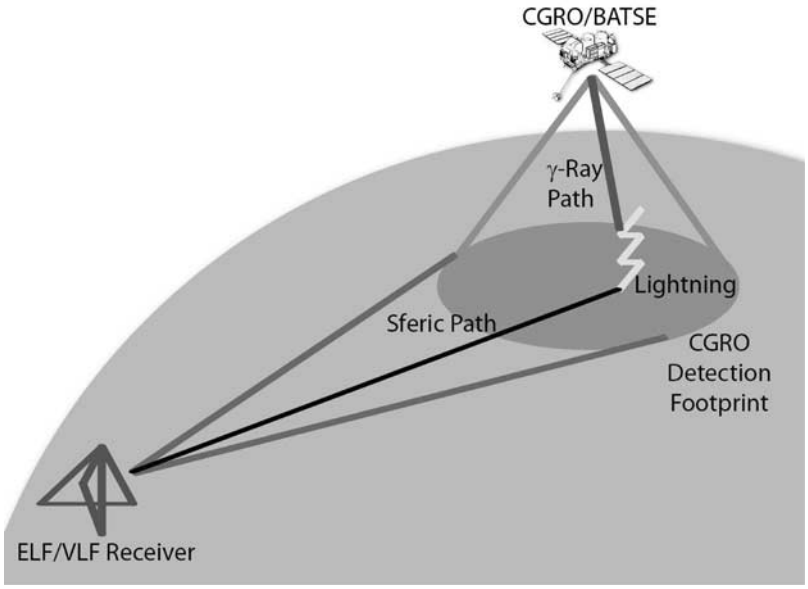

Figure 3. Geometry of TGF-sferic detection with VLF data. Both the propagation delays must be accounted for. The line-of-sight footprint of BATSE is 1350 km radius.

[15] The asymmetry of the mean with respect to zero is caused by the fact that while the propagation time from the source region to CGRO is necessarily larger than that from the nadir point immediately below, the propagation time from other points in the source region to Palmer can be either smaller or larger than that from the nadir point. So a TGF occurring 100 km further from the receiver would have both a longer propagation time from the source to receiver, and a longer propagation from the time source to satellite, and these two effects add up. However, a TGF occurring 100 km nearer to the receiver would have a shorter propagation time from the source to the receiver, though still a longer propagation time from the source to the satellite. Thus the two effects cancel each other out. In other words, simply because of geometry, we can expect, on average, the sferics to arrive slightly before time-zero, even if the sferic and TGF were exactly time-coincident at the source.

4. Overview of Data Analysis

[16] The light curves of the six BATSE cases are shown in Figure 4, for each of the TGF events, sferics (if any) that might be in space/time association with the TGF are identified (i.e., arriving near time-zero and from the CGRO region). The waveforms for each of the six cases is shown in Figure 5.

[17] For each case, all sferics observed at Palmer Station within a 30 minute time span (of time-zero) are also sorted by arrival azimuth, since enhanced sferic activity from a particular direction is evidence of thunderstorm activity [*Wood and Inan*, 2002]. These histograms are shown in Figure 6, with the highlighted region corresponding to azimuths from the CGRO footprint. This is done in order to ascertain the presence of active thunderstorms.

[18] Additionally, each sferic which matches with a TGF is then compared, separately in terms of both ELF and VLF intensity, to other sferics arriving from the BATSE/CGRO detection footprint (i.e., from the same storm). Figure 7 shows the intensities (written as percentiles) for the BATSE cases presented.

[19] In the following, we discuss the cases of the six TGF events, with individual attention to the different results, so as to call attention to the differences, sometimes fundamental, that exist among the cases.

5. BATSE Events 3470 and 3474

[20] Event 3470 occurred when CGRO was at 1°S, 3°E, off the west coast of Africa. The TGF onset was at 09:38:56.7995 universal time (UT), corresponding to early morning local time, on 16 March 1995. Working backward, the speed of light propagation time from nadir point to CGRO is 1.5 ms. Hence, if the TGF occurred at 09:38:56.7995, then the gamma rays would have been generated at 09:38:56.7980. The great circle propagation time from source to Palmer Station is found to be 29.7 ms. We find that the expected arrival time (time-zero) of the TGF matched sferic is 09:38:56.8277 UT.

[21] Event 3474 triggered the BATSE detector while CGRO was once again off the coast of Africa (6°N, 3°W), on 18 March 1995. The occurrence time was 08:10:34:349 UT, once again during early morning local time. Time-zero for this case is determined to be 08:10:34.3788 UT. The BATSE TGF signature consists of two distinct peaks, with the second one slightly shorter in duration, but both of which have the same peak count rate. The calculations of time-zero correspond to the onset of the first peak.

[22] The Palmer ELF/VLF waveform indicated in the first and second panels of Figure 5 shows a prominent sferics located ~1.4 ms and ~2.9 ms before time-zero. The early arrival of the sferic is consistent with the TGF occurring slightly after the lightning flash; however, it is also possible

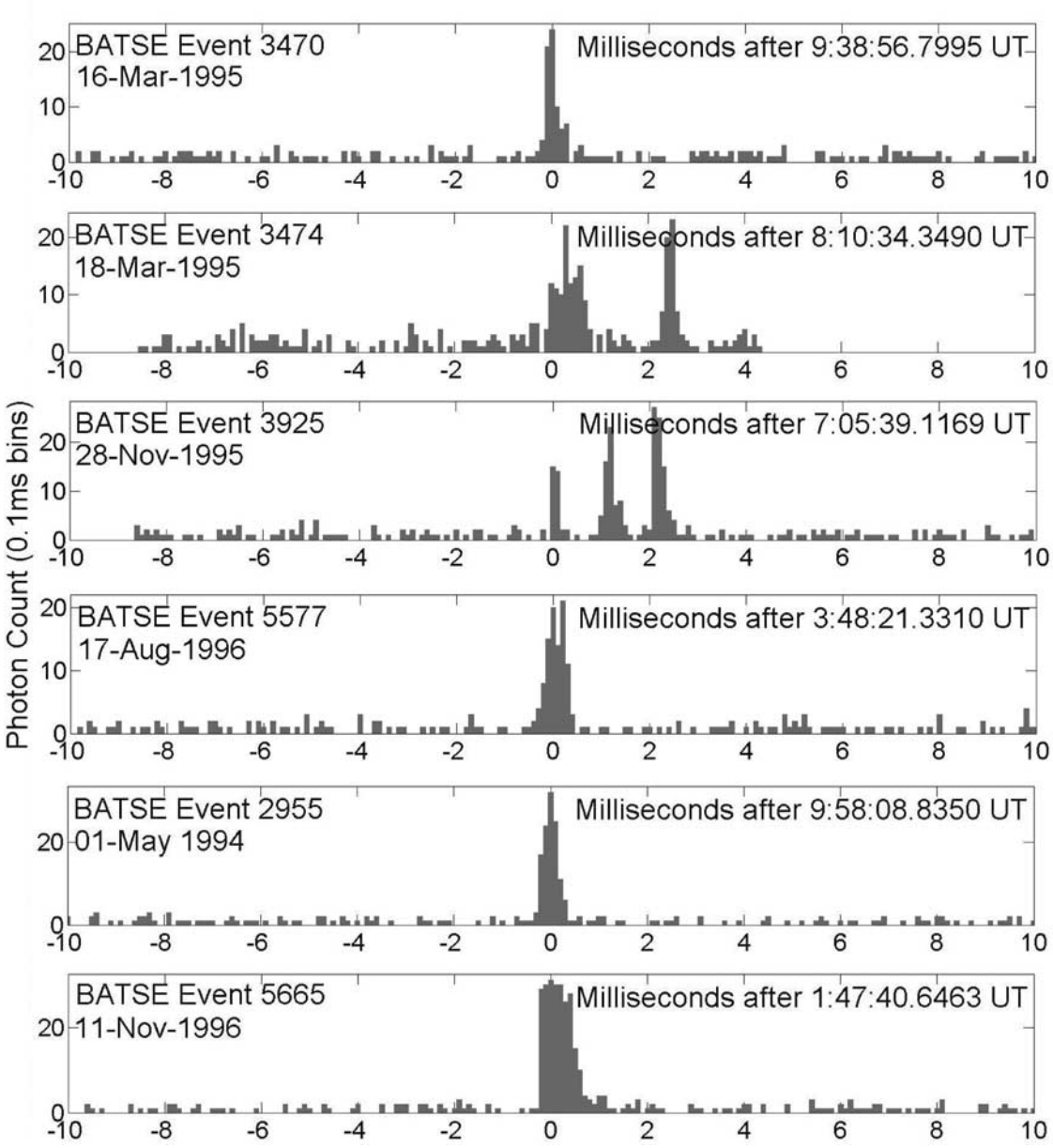

Figure 4. BATSE waveforms corresponding to the six TGF cases analyzed.

the sferic occurred at a location closer to Palmer than CGRO's nadir point. In each case, direction finding analysis applied to the causative sferic indicates that it originated from the east portion of the BATSE TGF detection footprint.

[23] Examining the arrival azimuths in Figure 6, there is a moderate peak or heightened activity in the azimuth range corresponding to the BATSE coverage region, even though with the BATSE/CGRO footprint at a relatively large distance from Palmer (~12000 km), many sferics produced in a likely thunderstorm may simply have fully attenuated before they reach Palmer. Hence, although it is thus difficult to definitively determine the presence of an active thunderstorm from such distances, the relative rarity of sferics coming from that region makes the occurrence of one so close to time-zero a statistically significant result. For event 3470, given that an average of 1.04 sferics per second were detected from the detection footprint, and assuming the occurrence of sferics to have a Poisson distribution, the probability of detecting one, by chance, from within BATSE's footprint, and within a 10 ms window of time-zero, is ~1%. The arrival rate for event 3474 was 1.4, hence the probability of chance occurrence is only ~1.1%

[24] On the basis of their ranking in terms of VLF and ELF intensities, each sferic can then be assigned a percentile rating value, with 99th percentile (for example) indicating it to be among the strongest 1% of sferics, while 1st percentile indicates that it is among the smallest 1%, when compared to others from within the detection circle. As seen in Figure 7, the sferic associated with these two TGF are particularly strong in terms of VLF intensity, but as much in terms of ELF energy. This is consistent with the presence of cloud to ground lightning strikes, since a higher VLF/ELF energy ratio has been tied to a more vertical source orientation [*Wood and Inan*, 2002] like what exists in a CG lightning stroke. It is

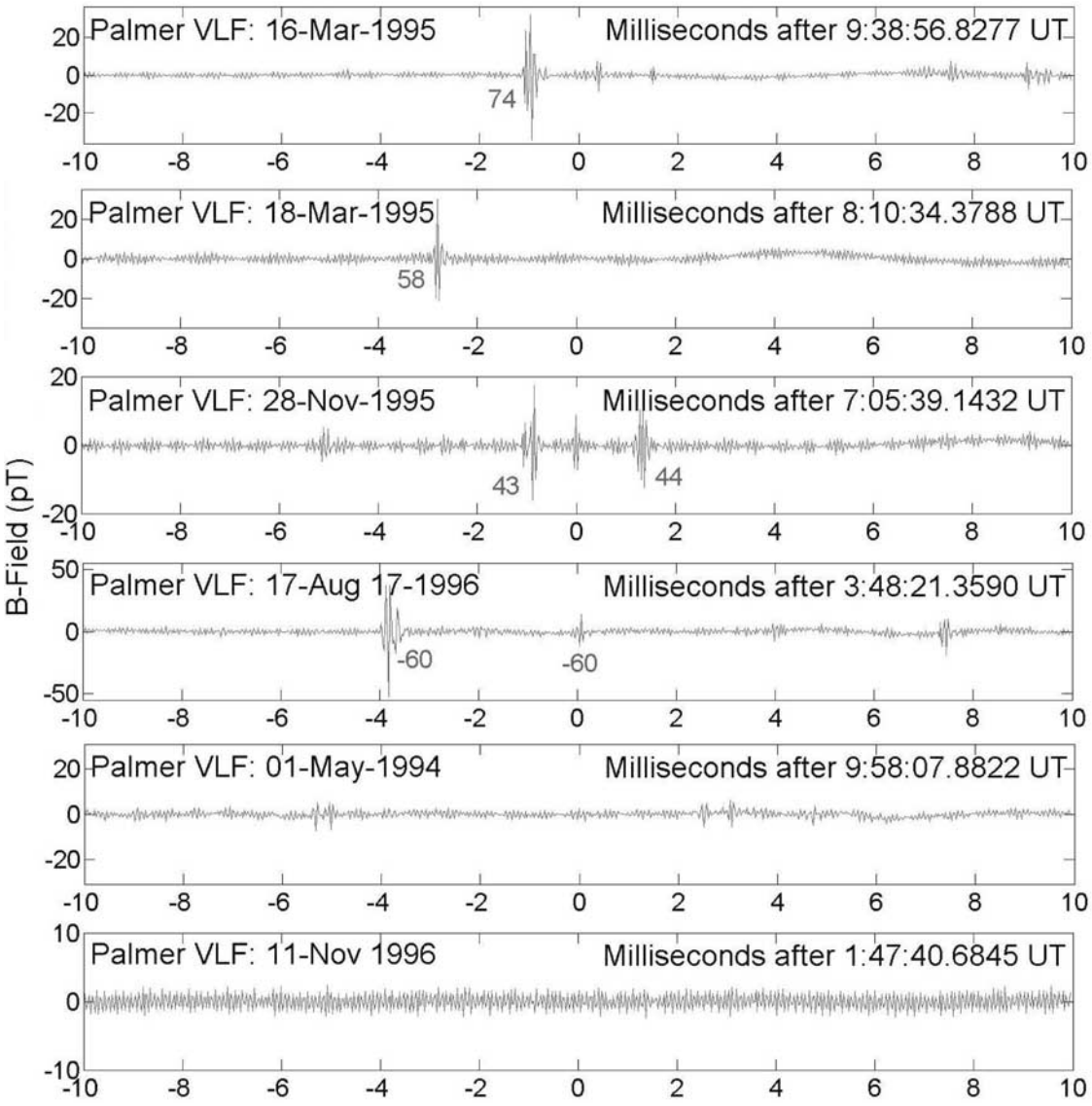

Figure 5. ELF/VLF waveforms corresponding to the six TGF cases analyzed.

also consistent with the theory of TGFs generated by lightning-EMP [*Inan and Lehtinen*, 2005].

[25] These two cases thus reconfirm the association between BATSE TGFs and lightning flashes that was observed for the case of TGF event 2348 analyzed by *Inan et al.* [1996]. The only qualitative difference is that the sferics here do not exhibit noticeable slow tails, whereas the one associated with 2348 did.

6. BATSE Event 3925

[26] Event 3925 occurred over the Atlantic Ocean (2°N, 18°W), sufficiently far enough from the coast of Africa that most of the detection footprint is over the ocean. The sferic propagation distance to Palmer is smaller than the first two examples (8300 km), but is still fairly large. As in event 3474, BATSE data exhibits multiple gamma ray spikes, in this case three, separated by ~1.5 ms each. Each successive peak is longer in duration and more intense than the previous one.

[27] Remarkably, the three pulses in the BATSE plot appear to correspond to three separate sferics, occurring at −1.1 ms, −0.1 ms, and 1.6 ms, with respect to time-zero (07:05:39.1433 UT). Direction finding analysis indicates that all three sferics originate from the detection footprint, arriving with azimuths 51.9°, 42.5°, and 44.8°, respectively (the detection footprint includes azimuths 48.8° +/ 12°). The sferic rate originating from the detection circle was ~2 per second, so that the probability of finding one sferic by chance within the 10 ms period is ~2.0%. The probability of finding at least three is truly minuscule, ~1.3 × 10E-6.

[28] As seen in Figure 7, these three sferics are not particularly large compared to others arriving from the same storm. The ELF energy content as defined here requires integration over a time period of >4 ms, and thus cannot be calculated for cases when multiple sferics occur close

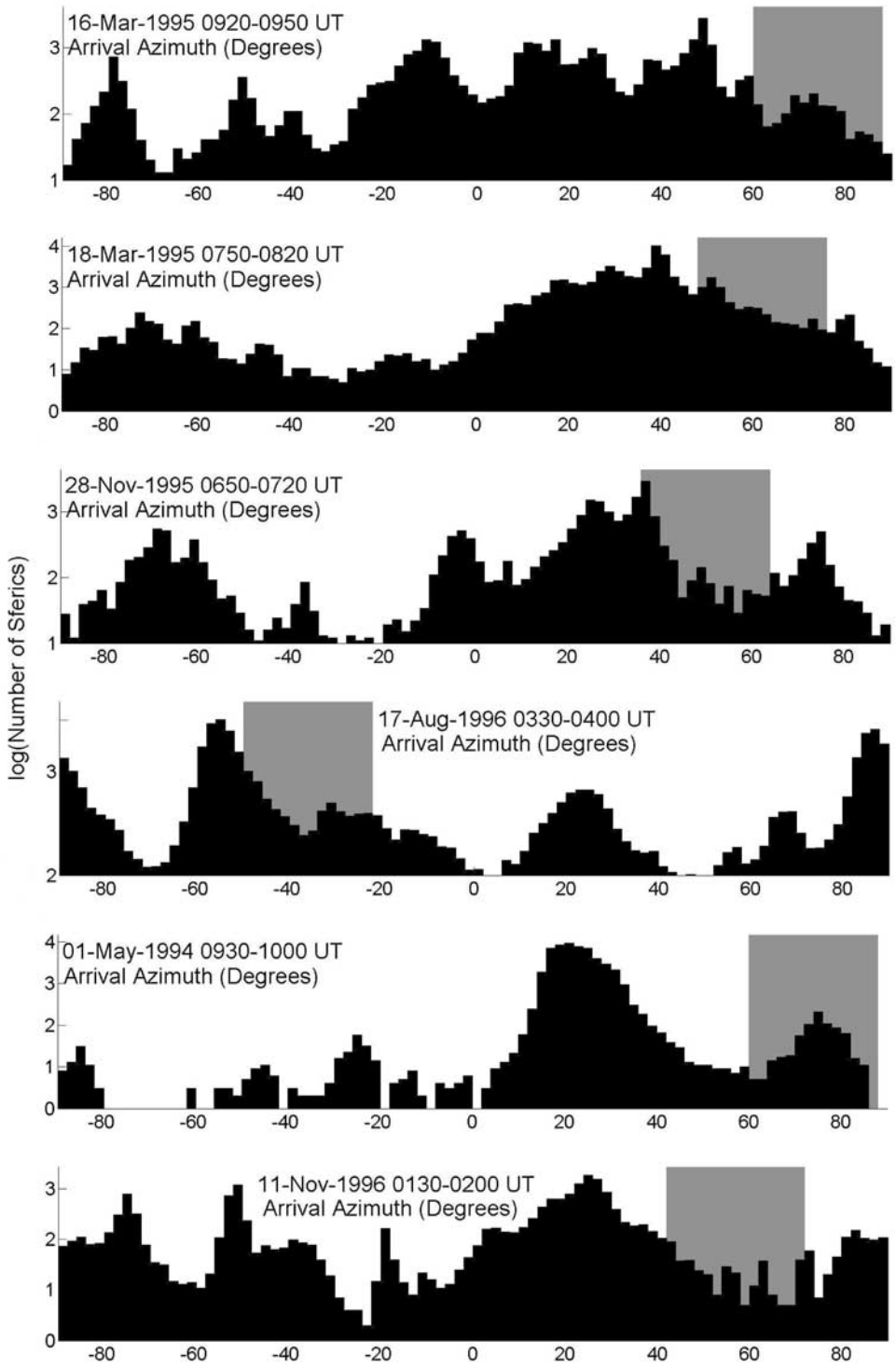

Figure 6. All sferics over a 30-min period centered at time-zero sorted by arrival azimuth. The shaded region indicates azimuths corresponding to the CGRO footprint. Elevated areas indicate evidence of active thunderstorms.

together [*Reising et al.*, 1996]; however, the three sferics do together exhibit a slow tail appearing primarily on the NS channel, so the ELF content here visibly appears to be stronger than 3470 and 3474.

[29] Currently, none of the proposed mechanisms for TGF production accounts for multiple peaks that are recorded on some BATSE TGF cases as a single event. The most spectacular example of these occurred on 1 March

Case	Arrival Time	VLF Energy	ELF Energy
3470	-1.4 ms	90	34
3474	-2.9 ms	55	23
3925*	-1.1 ms	51	***
5577**	-4.8 ms	31	91

* Largest of three sferics used
** Under conjugate TGF assumption
*** Cannot be determined

Figure 7. Each sferic matched to a TGF compared to others from the same direction during the same 30-min period and given a percentile both for ELF and VLF energy. 99th percentile indicates that the sferic was among the strongest 1%.

2000, namely BATSE event 8006, exhibiting at least 7 distinct peaks in the photon data, separated by ~2 ms each, as shown in Figure 8. Unfortunately, no VLF data was available for event 8006. Nevertheless, the event was observed as the CGRO passed immediately over a cyclonic thunderstorm in Darwin, Australia, which was an extremely active storm, lasting for many hours.

[30] The association between a group of three sferics and the three consecutive TGFs observed in event 3925 suggests the possibility that at least some of the multiple TGF peaks observed in some BATSE events (of which event 8006 is a spectacular example) may in fact be separate events, driven by separate (successive) lightning discharges. It is harder to imagine, however, that event 8006 was actually seven separate TGFs (driven by seven separate discharges), due to the unusually large number of consecutive peaks, and their nearly periodic nature. Experimental evidence for such events are difficult to find, on the basis of RHESSI observation that multiple-peak TGFs account for only ~1% of all TGFs (D. M. Smith, personal communication, 2005). BATSE triggering threshold scheme was somewhat biased toward capturing multiple-peak sferics because of the 64 ms integration time.

7. BATSE Event 5577

[31] Event 5577 was detected over the Atlantic Ocean, southwest of Mexico, at a location similar to that of event 2348 analyzed by *Inan et al.* [1996]. Although several sferics are visible in the VLF data, none of these arrive from directions to the BATSE detection footprint, even if the detection footprint is doubled in radius. The arrival azimuth histogram shows less evidence of an active thunderstorm at CGRO's location.

[32] The lack of sferics arriving from the nadir footprint of CGRO raises the question of the possibility that this event may be due to a lightning flash occurring in the geomagnetically conjugate region, as predicted by *Lehtinen et al.* [2001]. An investigation into the possibility of a conjugate TGF yields some evidence that the source of the TGF may in fact be located near the conjugate point, in which case the gamma rays detected by CGRO would have been launched by the electron beam as it impinges on the conjugate ionosphere from above and would thus reach the CGRO upon Compton scattering from the atmosphere. When the north-to-south propagation (along the magnetic field lines) of the highly relativistic (10 MeV) electron beam is taken into account (23 ms), the new "time-zero" is determined to be 3:48:21.3243 UT. Figure 9 shows the same VLF data, recalculated under these new assumptions.

[33] The sferic that arrives 4.8 ms before conjugate time-zero has an arrival azimuth of 73.8°, to be compared with the conjugate footprint encompassing the azimuths from 80.4° to 42.5°. The VLF intensity percentile of this sferic is 31, while its ELF energy content is in the 91st percentile. Although *Lehtinen et al.* [2001] predict that an extremely large charge moment (and thus ELF energy) would be required for electrons to escape, it is notable that the sferic associated with this case looks qualitatively the most like that which we would expect for a conjugate TGF, in comparison with other events presented here.

[34] In this case, the rate of arrival of sferics from the (conjugate) detection footprint is a much higher 6.5 per second (because of the fact that this thunderstorm is closer), meaning that random (by chance) occurrence of a sferic in a

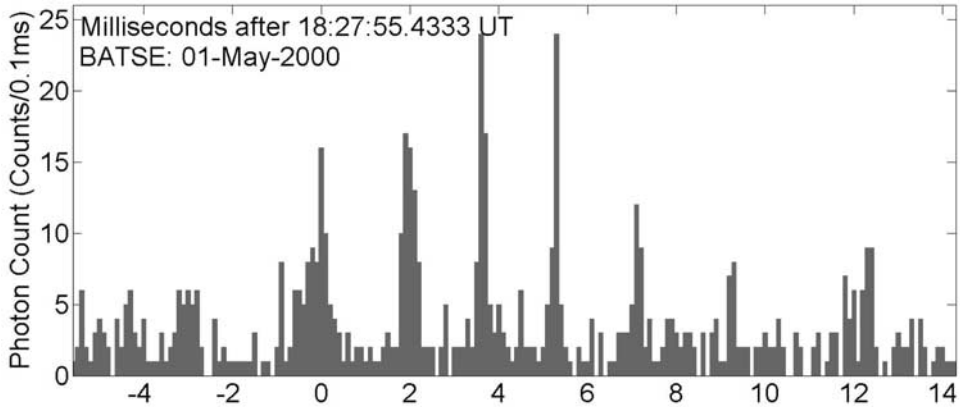

Figure 8. Most remarkable signature of BATSE event 8006, for which no VLF data were recorded.

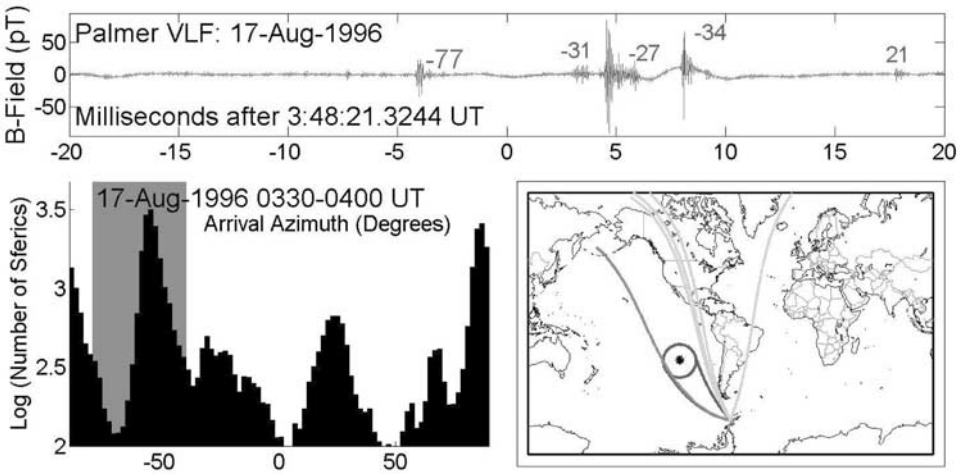

Figure 9. Event 5577 reexamined under the assumption of a geomagnetically conjugate source location.

10 ms span is 6.3%, once again assuming a Poisson arrival process. Because the conjugate CGRO location is much closer to Palmer Station, we can expect that any thunderstorm would be visible clearly in the histogram of arrival azimuths, as a peak at the corresponding azimuth range. The histogram does indeed show this.

[35] Finally, the spectral content of event 5577 provides some further evidence of a conjugate event. Whereas ~65% of TGFs observed by BATSE had the greatest intensity in the highest of its four energy channels (>323.06 keV), this TGF in fact had a stronger count in the second highest channel (106.65–323.06 keV). *Lehtinen et al.* [2001], however, predict that the third highest of four channels (57.83–106.65 keV) would see the largest count (36%), with a slightly smaller number (31%) in the second highest channel. Hence, while event 5577's spectrum is not completely in line with those calculations, the observed spectrum is closer to that predicted for conjugate events than are most BATSE TGFs.

8. BATSE Events 2955 and 5665

[36] For both cases, no associated sferic could be found within 10 ms of time-zero, originating from anywhere within the detection footprint, even if the detection footprint radius were doubled. The conjugate location, accounting for all propagation times, was also checked, but no matching sferic came within 20 ms of time-zero. There is however, strong evidence of an active thunderstorm underneath the CGRO in both cases. When all the sferics arriving over a 30 minute span are sorted, by arrival azimuth, we see a noticeable peak in the histogram at the azimuths corresponding to CGRO, for both of the cases.

[37] There are a number of possible explanations for a lack of sferic with the same time coincidence as in the other events. The causative lightning burst may not have been strong enough to generate a sferic that was detectable at Palmer Station. Alternatively, the TGF may have occurred in association with a lightning discharge that did not efficiently launch qTE and qTM modes in the Earth-ionosphere waveguide, such as a distant intracloud (IC) lightning flash.

[38] Alternatively, the TGF may have been generated by a physical process which either leads to a TGF long after a lightning discharge, or one that is not associated at all by a lightning discharge but is rather related to the presence of electrified (charged) thunderclouds as are present in active thunderstorms. In this context, it is interesting to note that the so-called gigantic jets, extending from thundercloud tops to the ionosphere [*Pasko et al.*, 1996; *Su et al.*, 2003] are observed to occur in the absence of any evidence for associated lightning discharges. It should be noted here that similar analysis of a large number of RHESSI TGFs also reveals a statistically significant number of cases with evidence of a thunderstorm under the spacecraft but no specific associated sferic matched in time with the TGF [*Inan et al.*, 2006].

9. Lightning-TGF Timing

[39] In total, of the eight TGF cases presented between this paper and *Inan et al.* [1996], four had associated sferics occurring within 5 ms of time-zero, based on the time of observation of the TGF, and accounting for propagation time, at Palmer Station, Antarctica. A fifth case is possibly explainable as a geomagnetically conjugate TGF. This result confirms a tight temporal coincidence (within a few ms) between at least the majority of TGFs and their associated sferics, unlike sprites, which may delayed by up to 100 ms from the lightning flash [*Uman*, 1987; *Reising et al.*, 1996].

[40] However, the exact nature of the lightning-TGF timing is currently a subject of debate. Many of the physical processes associated with large electric fields at high altitudes are associated with the return stroke of the lightning, in which case the TGF would slightly follow the lightning stroke. In contrast, TGFs associated with lower altitude processes may be consistent with x-ray and gamma ray observations made on the ground, in which case the lightning may slightly follow the TGF [*Dwyer et al.*, 2005].

[41] The timing of the three sferics matched to TGFs, plus the one from *Inan et al.* [1996] suggest that the TGF coincides with or immediately follows the causative sferic. Event 2348 from *Inan et al.* [1996] was reexamined using the same analysis tools that were used for the new cases

presented herein. Its causative sferic was found to be 4.5 ms prior to time-zero (a propagation time calculation error in the original paper caused the sferic to reported as 1.4 ms prior to time-zero, when it was in fact 4.5 ms before time-zero). Thus the sferics for the four matching cases (excluding the possible conjugate TGF) occur, in chronological order, −4.5 ms, −1.4 ms, −2.9, and −1.1 ms relative to time-zero, thus establishing a mean time delay of −2.5 ms. As discussed earlier, the geometrical variances would cause the sferic to arrive earlier than time-zero by 0–0.75 ms on average. Hence evidence in hand suggests that TGFs follow the lightning stroke by ∼1–3 ms, even though the number of events is small.

[42] Recent analysis of a larger number of RHESSI TGF cases has shown that the causative sferics occur shortly after time-zero. *Cummer et al.* [2005] found that the mean sferic arrival time was 1.24 ms late, from a survey of 26 TGFs in the Caribbean, 13 of which had causative sferics detected, using similar search criteria to those chosen here. Results from an analysis of >100 RHESSI TGF cases with Stanford University Palmer Station data, 88 of which have matching sferics, show an approximately Gaussian sferic arrival time distribution that has mean of 0.8 ms after time-zero and a sigma 2.4 ms [*Inan et al.*, 2006]. This finding corroborates (though slightly reduces) the average late arrival times mentioned by *Cummer et al.* [2005], for a much larger number of globally spread cases. Ostensibly, this would suggest that TGFs may precede sferics. The small sample or student t-test performed between the BATSE population of arrival times, and the RHESSI population of arrival times, show that the probability of this result, assuming the null hypothesis, is 0.0072. Hence it is highly likely the two clocks are offset with respect to each other. To 90% confidence, this offset between the two clocks is between 1.3 and 5.4 ms, established using the aforementioned small sample student t-test.

[43] However, the timing of the RHESSI clock is elsewhere believed to be unknown to about ∼3 ms, as recent comparisons to other spacecrafts [*Stanley et al.*, 2006] suggest a 3 ms offset. In this connection, we note that the absolute timing accuracy of BATSE TGF events is believed to be ∼0.1 ms. This accuracy was accomplished by linking the BATSE onboard computer clock with the spacecraft clock, which had an absolute time accuracy specification of 0.1 ms. The timing accuracy was attained throughout the mission with the use of a highly stable onboard clock and periodic updates by ground command, as needed. An independent means of checking the absolute timing accuracy was through the observation of pulsars with BATSE and other experiments on the Compton Gamma Ray Observatory.

[44] The suggestion here that TGFs follow the production of the sferic is consistent with models of TGF production associated with high electric fields during or shortly after the return stroke of the lightning.

10. Summary

[45] Although our analysis was necessarily limited to a modest number of events, a most interesting observation is that the cases presented herein reveal a wide range of fundamental differences in association of TGFs with lightning discharges. Events 3470 and 3474 are both equatorial cases, the associated sferics for which have stronger VLF than ELF content. However, events 3925 and 5577 (the one possible conjugate match) show much stronger ELF energy than VLF. The final two cases, 2955 and 5665, show no correlated sferic at all, despite evidence of thunderstorm activity, providing evidence that unusually weak CG lightning or IC lightning may also generate TGFs, or that TGFs may sometimes be produced with no accompanying lightning discharges, or a long time separation (>15 ms) before or after the lightning flash. Looking overall at the six cases, no pattern emerges. The widely disparate nature of the TGF-sferic connection in the CGRO cases points to the possibility that there may be multiple physical mechanisms responsible for generation of TGFs. Analysis of the timing of the sferics indicates that TGFs follow the causative sferic by 1–3 ms, in contrast with nominal results from the RHESSI instrument [*Cummer et al.*, 2005] and consistent with suggestions of an offset in the RHESSI clock (D. M. Smith, private communication, 2005). The relative weakness of results that occur from a study of a small number of events, however, still leave open questions that shall be answered when a much larger number of TGF events are carefully analyzed.

[46] **Acknowledgments.** This work was carried out with support from the National Science Foundation under grant OPP-0233955. We thank Troy Wood and Ryan Said for their help at various stages of data analysis.

References

Cummer, S. A., and U. S. Inan (1997), Measurement of charge transfer in sprite-producing lightning using ELF radio atmospherics, *Geophys. Res. Lett.*, *24*(14), 1731–1734.

Cummer, S. A., Y. Zhai, W. Hu, D. M. Smith, L. I. Lopez, and M. A. Stanley (2005), Measurements and implications of the relationship between lightning and terrestrial gamma ray flashes, *Geophys. Res. Lett.*, *32*, L08811, doi:10.1029/2005GL022778.

Cummins, K. L., M. J. Murphy, E. A. Bardo, W. L. Hiscox, R. B. Pyle, and A. E. Pifer (1998), A combined TOA/MDF technology upgrade of the U.S. National Lightning Detection Network, *J. Geophys. Res.*, *103*, 9035–9044.

Davies, K. (1990), *Ionospheric Radio*, Peter Peregrinus, London.

Dwyer, J. R., et al. (2005), X-ray bursts associated with leader steps in cloud-to-ground lightning, *Geophys. Res. Lett.*, *32*, L01803, doi:10.1029/2004GL021782.

Fishman, G. J., et al. (1994), Discovery of intense gamma-ray flashes of atmospheric origin, *Science*, *264*, 1313–1316.

Inan, U. S., and N. G. Lehtinen (2005), Production of terrestrial gamma-ray flashes by an electromagnetic pulse from a lightning return stroke, *Geophys. Res. Lett.*, *32*, L19818, doi:10.1029/2005GL023702.

Inan, U. S., S. C. Reising, G. J. Fishman, and J. M. Horack (1996), On the association of terrestrial gamma-ray bursts with lightning and implications for sprites, *Geophys. Res. Lett.*, *23*(9), 1017–1020.

Inan, U. S., M. B. Cohen, R. K. Said, D. M. Smith, and L. I. Lopez (2006), Terrestrial gamma ray flashes and lightning discharges, *Geophys. Res. Lett.*, *33*, L18802, doi:10.1029/2006GL027085.

Lehtinen, N. G., U. S. Inan, and T. F. Bell (2001), Effects of thunderstorm-driven runaway electrons in the conjugate hemisphere: Purple sprites, ionization enhancements, and gamma rays, *J. Geophys. Res.*, *106*(A12), 28,841–28,856.

Pasko, V. P., U. S. Inan, and T. F. Bell (1996), Blue jets produced by quasi-electrostatic pre-discharge thundercloud fields, *Geophys. Res. Lett.*, *23*(3), 301–304.

Reising, S. C., U. S. Inan, T. F. Bell, and W. A. Lyons (1996), Evidence for continuing currents in sprite-producing cloud-to-ground lightning, *Geophys. Res. Lett.*, *23*(24), 3639–3642.

Smith, D. M., L. I. Lopez, R. P. Lin, and C. P. Barrington-Leigh (2005), Terrestrial gamma-ray flashes observed up to 20 MeV, *Science*, *307*, 1085–1088.

Stanley, M. A., X.-M. Shao, D. M. Smith, L. I. Lopez, M. B. Pongratz, J. D. Harlin, M. Stock, and A. Regan (2006), A link between terrestrial

gamma-ray flashes and intracloud lightning discharges, *Geophys. Res. Lett.*, *33*, L06803, doi:10.1029/2005GL025537.

Su, H. T., et al. (2003), Gigantic jets between a thundercloud and the ionosphere, *Nature*, *423*, 974–976.

Uman, M. (1987), *The Lightning Discharge*, Elsevier, New York.

Wilson, C. T. R. (1925), The electric field of a thundercloud and some of its effects, *Phys. Soc. London Proc.*, *37*, 32D.

Wood, T. G., and U. S. Inan (2002), Long-range tracking of thunderstorms using sferic measurements, *J. Geophys. Res.*, *107*(D21), 4553, doi:10.1029/2001JD002008.

Wood, T. G., and U. S. Inan (2004), Localization of individual lightning discharges via directional and temporal triangulation of sferic measurements at two distant sites, *J. Geophys. Res.*, *109*, D21109, doi:10.1029/2004JD005204.

M. B. Cohen and U. S. Inan, Space, Telecommunications, and Radioscience Laboratory, Stanford University, 350 Serra Mall, Stanford, CA 94305, USA. (mcohen@stanford.edu)

G. Fishman, NASA Marshall Space Flight Center, Huntsville, AL 35805, USA.